

Influence of surface tension, osmotic pressure and pores morphology on the densification of ice-templated ceramics*

Sylvain Deville[†], Guillaume Bernard-Granger[‡]

Laboratoire de Synthèse et Fonctionnalisation des Céramiques,
UMR3080 CNRS/Saint-Gobain, Cavaillon, FRANCE

Abstract

We attempt here to clarify the influence of the nature of the solvent on the ice-templating process, based on literature experimental results of porosity and suspension concentration. In particular, we compare the relative influence of surface tension, osmotic pressure and the pore size and radius of curvature on the densification of the green bodies. Variations of the osmotic pressure when changing the solvent can yield significantly different behaviour during the freezing stage and therefore significantly affect the densification behaviour, an effect not apparent when using the Shanti model. In addition, and equally important, a modification of the macropores morphology is induced by the evolution of the solvent crystals morphology, and resulting in smaller and more intricate crystals and macropores which facilitates the densification. The radius of curvature is probably also an essential parameter controlling the densification of ice-templated ceramics.

Keywords: Porosity, Sintering, Ice-templating

1 Introduction

The ice-templating process has attracted an increasing interest over the last few years, in particular in the field of porous ceramics¹. The porosity in these materials is templated by the solvent crystals, which are subsequently removed by sublimation to obtain a green body, which in turn can be densified by conventional sintering methods. The process share many similarities with the existing ceramic processing routes -such as slip casting or pressing-

*doi:10.1016/j.jeurceramsoc.2010.12.021

[†]email: sylvain.deville@saint-gobain.com

[‡]now with : CEA, Grenoble, FRANCE

from the point of view of particles packing in the green body. Nevertheless, some specificities of the process should be investigated with greater attention. In particular, the choice of the solvent, which can be made for pragmatic reasons such as a higher solidification temperature or the absence of specific equipment -e.g., a freeze-dryer- for solvent removal, can also have a great influence over the characteristics of the porous bodies obtained. The solvent plays a key role on the redistribution and packing of particles which occur during the solidification step. Here, we attempt to clarify the influence of the nature of the solvent on the process, based on literature data. In particular, we compare the relative influence of surface tension and the pore size and radius of curvature on the densification of the green bodies.

2 Results and Discussion

The nature of the solvent is one of the many parameters which can be selected or adjusted in the ice-templating process. Water is the most commonly used, for obvious practical reasons, but also for the unique directional lamellar morphologies it usually provides. Camphene has also attracted a lot of interest, since the solidification temperature is much higher and avoids the use of low temperatures, and sublimation of the camphene crystals can occur at room temperature and pressure. Other solvents or solvent mixtures have been considered, such as glycerol, dioxane or camphor-naphthalene. The relationships between the slurry concentration (in volume) and the total porosity for these solvents and many different materials are plotted in figure 1. Of course, a great dispersion of the values is observed, due to variations of the processing conditions, slurry formulation, nature and characteristics of the powders, and densification conditions. We can nevertheless already notice that the porosity seems to be systematically much lower when camphene is used, compared to samples processed with water. Interestingly, the total porosity is even lower with the glycerol or dioxane-water mix, although only a few reports can be found and data scattering -as observed for water and camphene- is unknown.

A first parameter to take into account is the volume change of the solvent during the solidification: the solidification of water leads to a slight volume increase, while camphene slightly shrinks. This effect alone can nevertheless not account for the magnitude of differences observed experimentally (complete densification in some cases).

The local density in the green body will depend on the particles redistribution and concentration behaviour during the solidification step. Only a few parameters should account for the characteristics of particle packing in the ice-templated porous bodies. Here we use the model developed by Shanti et al.², which has proved to be reliable so far. Particles are rejected by the growing crystals and concentrate in the intercrystal space, until the

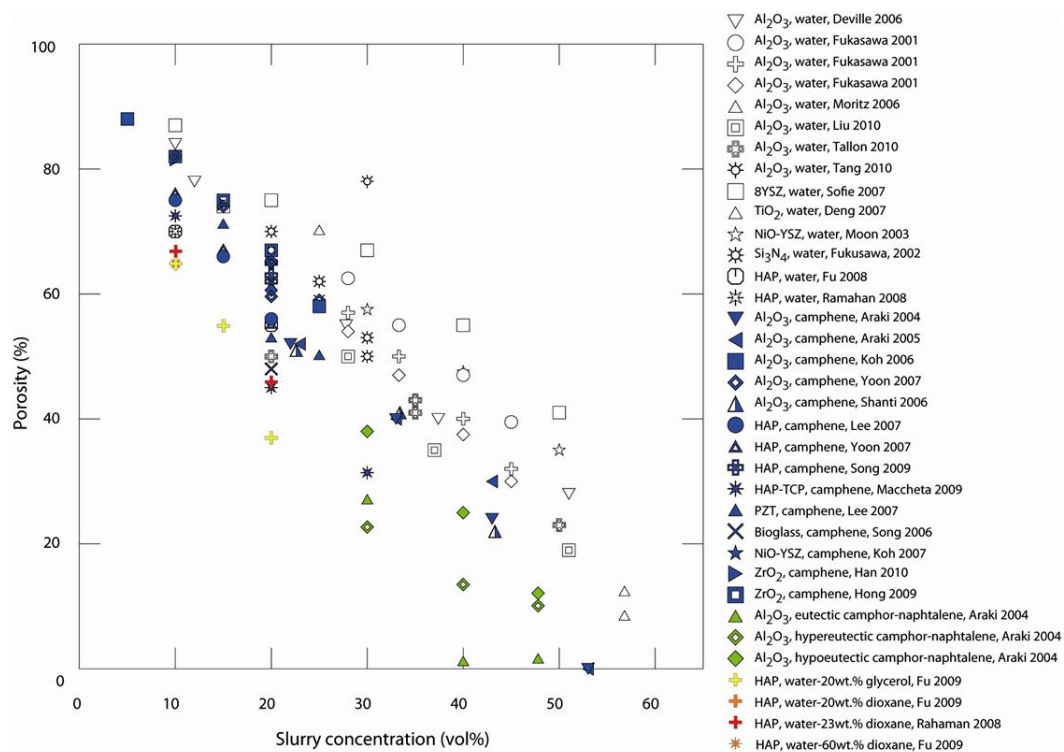


Figure 1: Total porosity vs. slurry concentration, literature data^{2,8-31}. The samples made with water, and camphene are respectively in white and dark. Other solvent are also represented, although fewer results can be found. The porosity of samples made with camphene is almost systematically lower than when made with water.

osmotic pressure exceeds the capillary pressure. At this point, the solid-liquid interface invades the interparticles space. The concentration at which this balance is lost is referred to as the breakthrough concentration. The breakthrough concentration therefore defines, after the sublimation step, the relative proportion of macropores, corresponding to pure ice crystals, and micropores, corresponding to the interparticle spaces in the concentrated particles regions between the pure ice crystals. If the breakthrough concentration is lower, the fraction of macropores is lower and the fraction of micropores is greater. This balance can be of great importance for densification, since micropores are easily removed during the sintering step. Let us first assume that the observed differences in densification behaviours originate from variations of the breakthrough concentration. The breakthrough concentration ϕ_b can be expressed as:

$$\phi_b = \phi_m - \left(\frac{kT}{4\pi R^2 \gamma} \right)^{\frac{1}{3}} \quad (1)$$

or

$$\phi_b = \phi_m - W \quad (2)$$

with

$$W = \left(\frac{kT}{4\pi R^2 \gamma} \right)^{\frac{1}{3}} \quad (3)$$

ϕ_m being the volume fraction of particles at maximum packing, T the temperature, R the particle radius (assuming particles are spherical) and γ the surface tension of the solvent. The only parameter of the solvent playing a role here is therefore the surface tension.

When plotting W vs. surface tension (fig. 2), water and camphene exhibits a very similar behaviour for usual particle sizes (0.2-1 μm). Variations of W become important for low surface tension and low particle size.

This is more clearly observed when plotting W vs. particle size, for water and camphene (fig. 3). The critical value of particle size, at which W becomes non-negligible ($> 1\%$), is around 300 nm for camphene and only 50 nm for water. Although the typical average particle size in commonly used ceramics powders is around 0.2-1 μm , the presence of a population of small particles ($< 100nm$) is almost systematic. It is also known that such a population of small particles, even if very limited, can have a tremendous influence over the osmotic pressure of colloidal suspensions³.

In our case, an increase of the osmotic pressure induces an important shift of the breakthrough concentration. We can therefore assume that in all cases, the breakthrough concentration will be lowered when the surface tension is lowered. The fraction of micropores in the green bodies processed with camphene should be greater than that of those processed with water. If we assume that this has a first order influence over the densification mechanism, since micropores are easily removed, a greater fraction of micropores

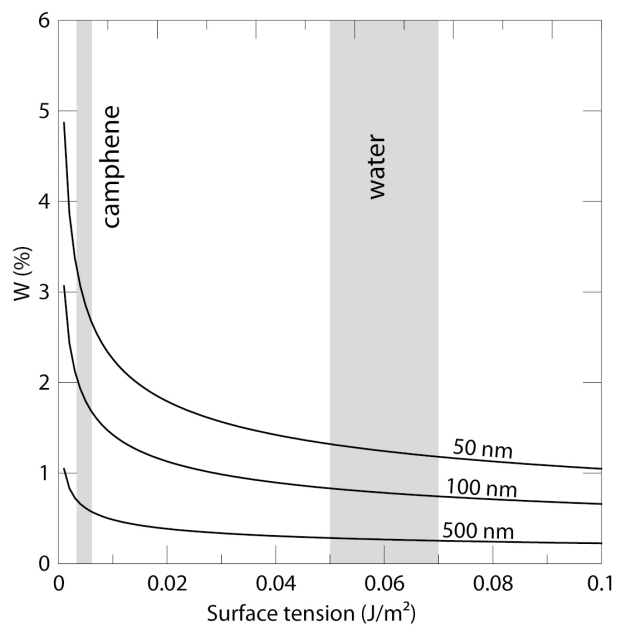


Figure 2: W vs. surface tension, for various particle sizes, and for a fixed temperature of 273K. The surface tension of water is very sensitive to the presence of impurities and usually lower than the value for pure water.

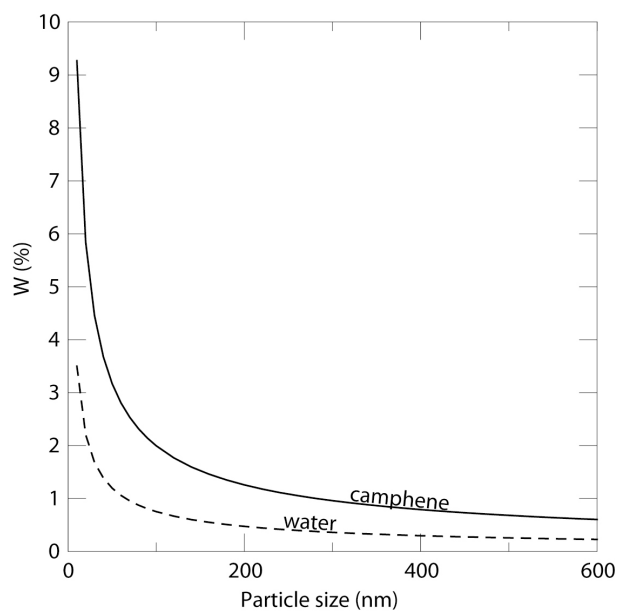


Figure 3: W vs. particle size, for camphene at 319K and water at 263 K

Solvent	Surface tension (N/m)
Water	0.07 to 0.03
Glycerol	0.065
Dioxane	0.03
Camphene	0.0044

Table 1: Surface tension of commonly used solvents³²

should make densification easier, so that we should expect lower porosity content with camphene or other low surface tension solvents. The experimental results are in good agreement with this theoretical result: porosity is systematically lower with camphene than with water. The differences in porosity between water-based and camphene-based materials are nevertheless too large to be accounted for only by the previously exposed reason. A variation of the surface tension, with the consequences previously exposed, should result in variation of the porosity of a few percent (typically 1 to 5%), no more, as shown in figure 2 and 3. The experimental data show that the variations in porosity can be as high as 20% with camphene, and even up to 40% with camphor-naphtalene. The balance between micropores and macropores is therefore probably not the most important parameter controlling the densification, according to the model of Shanti *et al.*

The Shanti paper, in deriving their expression for ϕ_b , actually neglects the effect of the solvent on the osmotic pressure of the colloidal particles. That solvent effects cannot be neglected is illustrated by measurements of the osmotic pressure of silica particles ($R=0.25\mu m$) dispersed in water (.01M NH_4Cl) and in toluene⁴. In toluene the osmotic pressure, at a given particle volume fraction, is found to be several orders of magnitude greater than in water. Thus changing the solvent can have a huge effect on the measured osmotic pressure. The analysis given in the Shanti paper cannot account for this effect as they use an expression for the osmotic pressure that is independent of the solvent, and is based on a hard-sphere equation of state. The solid-liquid surface energy of water varies from 0.07 to 0.03 N/m⁵, depending on its purity, while that for toluene is approximately 0.01 N/m⁶ (Table 1). Applying these values to the equation 1 yields (assuming $\phi_m = 0.64$):

$$\phi_b(\text{water}) = \phi_m - .006 = 0.634$$

$$\phi_b(\text{toluene}) = \phi_m - .008 = 0.632$$

Thus, according to the Shanti model, it would seem changing the solvent has little effect on the breakthrough concentration. However, as noted above the Shanti derivation neglects the effect of the solvent on the osmotic pressure. Instead of the Shanti equation one should use the more general equation of the osmotic pressure derived by White⁷ (assuming spherical particles) to determine ϕ_b :

$$\Pi = \frac{3\phi_b\gamma}{(1 - \phi_b)R} \quad (4)$$

where Π is the measured osmotic pressure. To determine ϕ_b from this equation one chooses ϕ_b until the left hand and right hand sides match. If we apply this equation to the experimental data of Guo⁴ we obtain:

$$\phi_b(\text{water}) = 0.63$$

$$\phi_b(\text{toluene}) = 0.4$$

Thus changing the solvent would significantly reduce the breakthrough concentration. This seems much closer to the values required in the camphene case to account for the variations of the experimental observations. One way to test this more general relation would be to determine the osmotic pressure of the colloidal particles when dispersed in both water and camphene, and the other solvents such as dioxane and glycerol. If they differ by several orders of magnitude, it is likely the more general White equation will yield significantly different breakthrough concentrations.

Finally, we propose here that an additional parameter is controlling the densification of the green bodies, that is, the local curvature of the solid interface. It is well established that the diffusion processes, associated to grain growth and densification during solid-state sintering of ceramic powders, are governed by the curvature of the interfaces (solid / vapour for densification, solid / solid for grain growth). The driving force is the pressure difference across the interface, DP, having the well known expression:

$$DP = \frac{2\gamma}{R} \quad (5)$$

with γ the surface energy of interest and R the radius of curvature of the interface. The lower the radius of curvature of the interfaces, the higher the driving force for grain growth and/or densification.

In the case of ice-templated ceramics, very different morphologies are obtained when different solvent are used¹. In particular, in the case of camphene, highly dendritic structures are obtained, therefore with a low radius of curvature of the interface. When using water, lamellar morphologies of greater pores dimensions and with a less intricate structure are obtained. In the case of glycerol and dioxane/water suspensions, the structures are even more intricate, with smaller and more dendritic pores. The experimental results summarized in figure 1 are in good agreement with this hypothesis. Green bodies with structures exhibiting a low local radius of curvature will facilitate the densification and yield porous structures with a lower porosity content, which is schematically represented in figure 4. For an equivalent initial slurry concentration, the final total porosity decreases when the low local radius of curvature decreases. For green bodies where the pores are very small and intricate⁸, the porosity can be completely removed by densification.

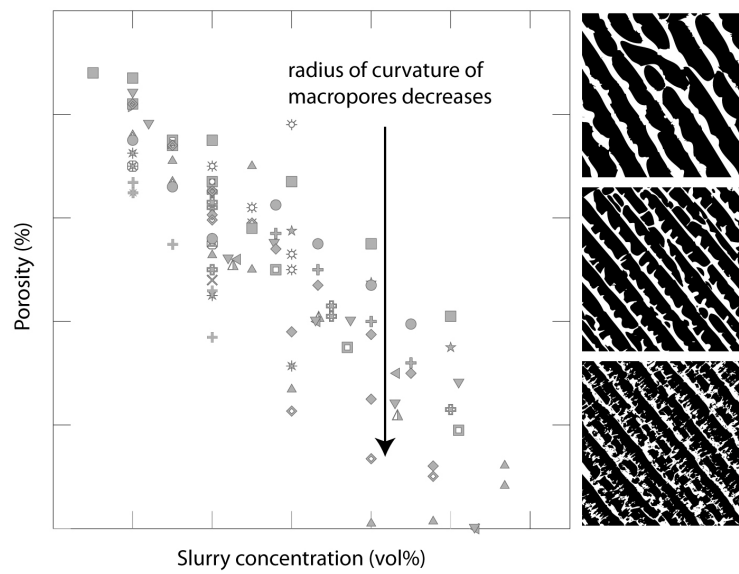


Figure 4: Total porosity vs. slurry concentration. The decrease of porosity, for a given slurry concentration, corresponds to a decrease of the radius of curvatures of the macropores, with typical structures schematically shown on the right.

3 Conclusions

Based on a review of the literature data and an analysis of the model developed by Shanti et al., we propose here that the densification of ice templated ceramics is governed both by the influence of the osmotic pressure during the solidification stage and by the morphology of the macropores, and more specifically the radius of curvature of the solid/vapour interface. The choice of a solvent for the process, such as water, camphene, dioxane or glycerol, will have a partial influence through the variation of the surface tension, which affects local particles packing and therefore the balance between macroporosity and microporosity, but this alone cannot explain the magnitude of porosity variations observed experimentally. The Shanti derivation neglects the effect of the solvent on the osmotic pressure. Instead of the Shanti derivation one should, for instance, use the more general equation of the osmotic pressure derived by White. Variations of the osmotic pressure when changing the solvent can yield significantly different behaviour during the freezing stage and therefore significantly affect the densification behaviour, an effect not apparent when using the Shanti model. In addition, and equally important, a modification of the pores morphology is induced by the evolution of the solvent crystals morphology when changing the solvent. Highly dendritic and small crystals will facilitate the densification of the green body and yield porous materials with a lower total porosity. Determination of the osmotic pressure in the typical ice-templating suspensions are required to validate these propositions.

References

1. S. Deville. Freeze-Casting of Porous Ceramics: A Review of Current Achievements and Issues. *Adv. Eng. Mater.* 2008;10[3]:155-169.
2. N. O. Shanti, K. Araki, and J. W. Halloran. Particle Redistribution During Dendritic Solidification of Particle Suspensions. *J. Am. Ceram. Soc.* 2006;89[8]:2444-2447.
3. M.-L. Rami, M. Meireles, B. Cabane, and C. Guizard. Colloidal Stability for Concentrated Zirconia Aqueous Suspensions. *J. Am. Ceram. Soc.* 2009;92[s1]:S50-S56.
4. J. J. Guo and J. A. Lewis. Aggregation Effects on the Compressive Flow Properties and Drying Behavior of Colloidal Silica Suspensions. *J. Am. Ceram. Soc.* 1999;82[9]:2345-2358.
5. P. V. Hobbs, "Ice Physics," pp. 864. Oxford: Oxford University Press. (2010).

6. M. Hatase, M. Hanaya, T. Hikima, and M. Oguni. Discovery of homogeneous-nucleation-based crystallization in simple glass-forming liquid of toluene below its glass-transition temperature. *J. Non-Cryst. Solids* 2002;307-310:257-263.
7. L. R. White. Capillary rise in powders. *J Colloid Interf Sci* 1982;90[2]:536-538.
8. K. Araki and J. W. Halloran. Room-Temperature Freeze Casting for Ceramics with Nonaqueous Sublimable Vehicles in the Naphthalene-Camphor Eutectic System. *J. Am. Ceram. Soc.* 2004;87[11]:2014-2019.
9. S. Deville, E. Saiz, and A. P. Tomsia. Ice-templated porous alumina structures. *Acta Mater.* 2007;55:1965-1974.
10. T. Fukasawa, M. Ando, T. Ohji, and S. Kanzaki. Synthesis of porous ceramics with complex pore structure by freeze-dry processing. *J. Am. Ceram. Soc.* 2001;84[1]:230-232.
11. T. Moritz and H.-J. Richter. Freeze casting of ceramic components using ice cores and ice molds. *Adv Sci Tech* 2006;45:391-396.
12. G. Liu, D. Zhang, C. Meggs, and T. W. Button. Porous Al₂O₃-ZrO₂ Composites Fabricated by an Ice Template Method. *Scripta Mater.* 2010;62[7]:466-468.
13. C. Tallon, R. Moreno, and M. I. Nieto. Shaping of porous alumina bodies by freeze casting. *Advances in Applied Ceramics* 2009;108[5]:307-313.
14. Y. F. Tang, K. Zhao, J. Q. Wei, and Y. S. Qin. Fabrication of aligned lamellar porous alumina using directional solidification of aqueous slurries with an applied electrostatic field. *J. Eur. Ceram. Soc.* 2010;30[9]:1963-1965.
15. S. W. Sofie. Fabrication of Functionally Graded and Aligned Porosity in Thin Ceramic Substrates With the Novel Freeze-Tape-Casting Process. *J. Am. Ceram. Soc.* 2007;90[7]:2024-2031.
16. Z.-Y. Deng, H. R. Fernandes, J. M. Ventura, S. Kannan, and J. M. F. Ferreira. Nano-TiO₂-Coated Unidirectional Porous Glass Structure Prepared by Freeze Drying and Solution Infiltration. *J. Am. Ceram. Soc.* 2007;90[4]:1265-1268.
17. J.-W. Moon, H.-J. Hwang, M. Awano, and K. Maeda. Preparation of NiO-YSZ tubular support with radially aligned pore channels. *Mater. Lett.* 2003;57[8]:1428-1434.

18. T. Fukasawa, Z. Y. Deng, M. Ando, T. Ohji, and S. Kanzaki. Synthesis of porous silicon nitride with unidirectionally aligned channels using freeze-drying process. *J. Am. Ceram. Soc.* 2002;85[9]:2151-2155.
19. Q. Fu, M. N. Rahaman, F. Dogan , and S. B. Bal. Freeze casting of porous hydroxyapatite scaffolds. I. Processing and general microstructure. *J. Biomed. Mater. Res. B* 2008;86B:125-135.
20. M. N. Rahaman and Q. Fu. Manipulation of Porous Bioceramic Microstructures by Freezing of Suspensions Containing Binary Mixtures of Solvents. *J. Am. Ceram. Soc.* 2008;91[12]:4137-4140.
21. K. Araki and J. W. Halloran. New freeze-casting technique for ceramics with sublimable vehicles. *J. Am. Ceram. Soc.* 2004;87[10]:1859-1863.
22. Y. H. Koh, I. K. Jun, J. J. Sun, and H. E. Kim. In situ fabrication of a dense/porous Bi-layered ceramic composite using freeze casting of a ceramic-camphene slurry. *J. Am. Ceram. Soc.* 2006;89[2]:763-766.
23. B.-H. Yoon, Y.-H. Koh, C.-S. Park, and H.-E. Kim. Generation of Large Pore Channels for Bone Tissue Engineering Using Camphene-Based Freeze Casting. *J. Am. Ceram. Soc.* 2007;90[6]:1744-1752.
24. J.-H. Song, Y.-H. Koh, H.-E. Kim, L.-H. Li, and H.-J. Bahn. Fabrication of a Porous Bioactive Glass-Ceramic Using Room-Temperature Freeze Casting. *J. Am. Ceram. Soc.* 2006;89[8]:2649-2653.
25. E.-J. Lee, Y.-H. Koh, B.-H. Yoon, H.-E. Kim, and H.-W. Kim. Highly porous hydroxyapatite bioceramics with interconnected pore channels using camphene-based freeze casting. *Mater. Lett.* 2007;61[11-12]:2270-2273.
26. Y.-M. Soon, K.-H. Shin, Y.-H. Koh, J.-H. Lee, and H.-E. Kim. Compressive Strength and Processing of Camphene-Based Freeze Cast Calcium Phosphate Scaffolds with Aligned Pores. *Mater. Lett.* 2009;63[17]:1548-1550.
27. A. Macchetta, I. G. Turner, and C. R. Bowen. Fabrication of HA/TCP scaffolds with a graded and porous structure using a camphene-based freeze-casting method. *Acta Biomater.* 2009;5[4]:1319-1327.
28. S.-H. Lee, S.-H. Jun, H.-E. Kim, and Y.-H. Koh. Fabrication of Porous PZT-PZN Piezoelectric Ceramics With High Hydrostatic Figure of Merits Using Camphene-Based Freeze Casting. *J. Am. Ceram. Soc.* 2007;90[9]:2807-2813.

29. Y. H. Koh, J. J. Sun, and H. E. Kim. Freeze casting of porous Ni-YSZ cermets. *Mater. Lett.* 2007;61[6]:1283-1287.
30. J. Han, C. Hong, X. Zhang, J. Du, and W. Zhang. Highly porous ZrO₂ ceramics fabricated by a camphene-based freeze-casting route: Microstructure and properties. *J. Eur. Ceram. Soc.* 2010;30[1]:53-60.
31. C. Hong, X. Zhang, J. Han, J. Du, and W. Han. Ultra-high-porosity zirconia ceramics fabricated by novel room-temperature freeze-casting. *Scripta Mater.* 2009;60[7]:563-566.
32. B. Bayander, N. Marasli, E. Chadirli, and M. Gunduz. Solid-liquid interfacial energy of camphene. *Mater. Sci. Eng., A* 1999;270:343-348.